The Academic
International Journal of Multidisciplinary Research

An Online Peer Reviewed / Refereed Journal
Volume 3 | Issue 12 | December 2025
ISSN: 2583-973X (Online)
Website: www.theacademic.in

Effect of SILAR Cycle on the Optical and Electrical Properties of SILAR Grown Copper Iron Sulphide Thin Films

T.O. Fowodu[1, 2*], Dibya Jyoti Borah[3]*, Kola Odunaike[2], Q.A. Adeniji[4], A.D. Adelaja[1], and A.T. Talabi[2]

[1]Department of Physics, Tai Solarin University of Education, Ijagun, Nigeria

[2]Department of Physics, Olabisi Onabanjo University, Ago-Iwoye, Nigeria

[3]Department of Physics, Majuli College, Majuli-785106, Assam, India

[4]Department of Physical and Chemical Sciences, Federal University of Health Sciences, Ila-Orangun,, Nigeria

*Corresponding author:

E-mail ID: temitopefowodu@gmail.com/ fowoduto@tasued.edu.ng (T.O. Fowodu)

jyotidibya2015@gmail.com (Dr. Dibya Jyoti Borah)

DOI : https://doi.org/10.5281/zenodo.18220160

ARTICLE DETAILS

Research Paper

Accepted: 19-12-2025

Published: 10-01-2026

Keywords:

Copper Iron Sulphide (CFS), SILAR cycle, negative refractive index, energy bandgap, thin films

ABSTRACT

Copper iron sulphide thin films tagged "CFS" were prepared on microscope glass slides to study the effect of SILAR cycle on the optical and electrical properties of the grown thin films using Successive Ionic Layer Adsorption and Reaction (SILAR) technique at room temperature (300 K) from aqueous solution of Iron(III) trioxonitrate nanohydrate, copper(II) chloride dihydrate, and thiourea as precursors with EDTA, TEA and NH_4OH as complexing agents at varied SILAR cycles (30, 40, and 50 cycles) of deposition. The thin films grown were characterized using Avalight-DH-S-BAL Avantes UV-VIS spectrophotometer in the wavelength range 200-1000 nm and Keithley 4ZA4 2400 sourcemeter equipped with a four-point probe setup. The optical properties of the films revealed high absorbance and reflectance but low transmittance in the UV region; low values of absorbance and reflectance accompanied with high transmittance in the VIS region. The extinction coefficient of the films increased with an increase in SILAR cycle and are very close to zero for wavelengths

940 nm and above for all the films. There was no refractive index in the UV-VIS regions and the maximum values of the refractive index for all the films are -1.70, -1.60, and -2.85 in increasing order of SILAR cycle at a wavelength of about 975 nm. From the Tauc plot, the study revealed that the energy band gap decreased from ~ 4.10-3.88 eV with the increase of SILAR cycle. Also, the electrical conductivity of the deposited films are found to increase with the increase of SILAR cycle.

1. Introduction

In recent years, the synthesis and study of chalcogenide compounds have increased owing to their remarkable properties and wide range of applications in various solid-state and optoelectronic devices. Thin films of these chalcogenide compounds possess numerous uses in opto-electronic devices, and window layer material in solar cells, and for this reason, ternary thin films are being studied extensively [1, 2, 3]. In addition to these, ternary chalcogenide thin films find potential applications in light-emitting diodes (LEDs) and non-linear optical devices [1]. Few researchers have successfully deposited and characterized copper iron sulphide (CFS) thin films using chemical bath deposition (CBD) [2, 3], solution growth technique (SGT) [4], and successive ionic layer adsorption and reaction (SILAR) [5]. SILAR technique is one of the chemical methods for making uniform and large area thin films, based on immersion of substrates into separately placed cation and anion sources. The edge of the SILAR technique is that it is very attractive, simple, easy, environmentally friendly, and possesses easy reproducibility in the field of solar cell fabrication due to its excellent material utilization efficiency, good control over the deposition process along with the film thickness, low-cost, and large-scale deposition capability on virtually any type of substrate. Many researchers have developed an interest in the preparation of ternary photovoltaic materials due to the potential of fashioning both the lattice parameters and the energy bandgap by influencing deposition parameters like the SILAR cycles.

To the best of our knowledge, the SILAR technique has not been employed to grow CFS, and there are hardly any reports on the fabrication of solar cells with CFS materials grown by the SILAR method. Therefore, in the present work, CFS thin films are fabricated at different SILAR cycles. And, the dependence of SILAR cycles on the optical and electrical properties of the CFS thin films is comprehensively investigated in the present research work. Various optical parameters, such as optical band gap, extinction coefficient, and refractive index, have been evaluated, and their correlation with the

number of SILAR cycles has been established.

2. Experimental section

2.1 Materials and methods

The reagents used for the study were of stoichiometric and analytical grade of Iron(III) trioxonitrate nanohydrate ($Fe[NO_3]_3.9H_2O$), Copper(II) chloride dihydrate ($CuCl_2.2H_2O$), and Thiourea ($[NH_2]_2CS$). Here, $Fe[NO_3]_3.9H_2O$, $CuCl_2.2H_2O$, and $(NH_2)_2CS$ were the precursors while ethylenediaminetetraacetate (EDTA) and triethanolamine (TEA) were the complexing agents with deionized water and ammonia solution (NH_4OH). Microscopic glass slide of dimensions 76.2 mm × 2.5 mm × 1.2 mm were used as substrates for thin film fabrication.

SILAR technique was employed in this study. CFS thin films were deposited on microscopic glass slide when immersed into the precursors and was carried out using four beakers system (Beakers I, II, III and IV) at room temperature (RT). In order to remove the organic and inorganic impurities on the glass, the substrates were thoroughly cleaned and degreased for 48 hours by soaking in hydrochloric and trioxonitrate(V) acids in the ratio of 3:1, respectively. The glass slides were rinsed in distilled water after degreasing and then dried in air giving the slides the advantage of providing nucleation centres for the growth of highly adhesive and uniformly deposited thin films.

Solutions of a four-beaker system were obtained by first preparing 5 mL of 0.7 M $Fe[NO_3]_3.9H_2O$, 5 mL of 0.7 M $CuCl_2.2H_2O$, 5 mL of 14 M ammonia solution, 5 mL of 7.4 M TEA, 5 mL of 0.1 M EDTA was placed into 50 mL beaker (Beaker I) and magnetically stirred at RT to obtain a homogenous solution. Then, 25 mL of deionized water was put into two different 50 mL beakers (Beakers II and IV). 25 mL of 1 M $[NH_2]_2CS$ was placed into another 50 mL beaker (Beaker III). The solutions in the beakers I and III served as cationic and anionic precursors. The $Fe[NO_3]_3.9H_2O$, $CuCl_2.2H_2O$, and $(NH_2)_2CS$ served as sources of Fe^{2+}, Cu^{2+}, and S^{2-}, respectively, while the TEA and EDTA served as complexing agents, slowed down the reactions for the formation of solid thin films on the substrates, whereas NH_4OH stabilizes the pH of the homogenous mixtures. The substrate was kept vertically in each beaker at every immersion to prevent it from slanting in the beaker. The deposition was carried out at RT for 120 seconds dip time per cycle.

One SILAR cycle consisted of four steps: adsorption of both Fe^{2+} and Cu^{2+} species for 30 seconds, rinsing with distilled water for 30 seconds to remove excess adsorbed or loosely bounded Fe^{2+} and Cu^{2+} species, reaction with $(NH_2)_2CS$ precursor solution for 30 seconds to form stable CFS and rinsing with

purified water for 30 seconds to remove excess or unreacted species or powdery CFS. By repeating such deposition cycle 30, 40, and 50 times, CFS thin films were obtained, respectively. After the deposition, the substrates were removed and allowed to air dry. The samples deposited at 30, 40 and 50 cycles were coded as CFS1, CFS2, and CFS3, respectively.

2.2 Characterizations

The films synthesized were characterized for optical reflectance (R) and transmittance (T) using Avalight-DH-S-BAL Avantes UV-VIS spectrophotometer. Other properties such as film absorbance (A), absorption coefficient (α), thickness (t), band gap energy (E_g), extinction coefficient (k) and refractive index were obtained theoretically from the values of reflectance and transmittance obtained. These optical properties were obtained in the wavelength range of 250 – 1000 nm.

The absorbance (A) was obtained using the relation [6];

$$A = 2 - log \log_{10} T \quad (1)$$

where, T is the transmittance.

The absorption coefficient (α) was determined using Lambert equation [6]:

$$\alpha = 2.303 \frac{A}{t} \quad (2)$$

where, A is the absorbance, t is the estimated film thickness ($t = 0.2\,nm$) obtained from gravimetric (weight gain) method [6];

$$t = \frac{M}{\rho S_a} \quad (3)$$

where, M represents the mass of the thin films deposited on the surface of the microscopic glass slide, obtained from the expression $M = m_2 - m_1$. Here, m_1 is the mass of the glass slide before film deposition, m_2 is the mass weighted by the glass slide after film deposition, ρ is the average of the bulk densities (gcm^{-3}) of CuS and Fe and S_a is the surface area of the thin films on the substrate.

The photon energy E, is given by equation [6]:

$$E = h\nu \quad (4)$$

$$\nu = \frac{c}{\lambda} \quad (5)$$

where, $h = 6.626 \times 10^{-34} Js^{-1}$ (Planck's constant), ν is the frequency of the photon, $c = 3 \times 10^{8}\ ms^{-1}$ (velocity of light) and λ is the wavelength of the photon.

The energy band gaps (E_g) of the obtained films were extrapolated from the Tauc plot relation given by [7]:

$$\alpha = \frac{A}{h\nu}(h\nu - E_g)^n \quad (6)$$

where, A is the parameter that depends on the transition chance, and n is the value that depends on the transition type. The number $n = 2$ denotes direct band gap transition and $n = \frac{1}{2}$ denotes indirect band gap transition. For the determination of the band gap, the direct ($n = 2$) transitions were considered. The resulting plot has a distinct linear segment that indicates the beginning of the light absorption spectra. The intersection of the extrapolated linear part with the abscissa axis shows the band gap, E_g value. Extrapolating the linear region to the abscissa yields the energy of the optical band gap of the material.

Extinction coefficient k, is a measure of the fraction of photon energy loss due to scattering and absorption. The extinction coefficient of the thin films was determined using the relation [6];

$$k = \frac{\alpha\lambda}{4\pi} \quad (7)$$

where, α is the absorption coefficient (attenuation coefficient) and λ is the incident photon wavelength.

The refractive index (η) of the thin films was calculated using the expression given by [8]

$$\eta = \frac{1 + \sqrt{R}}{1 - \sqrt{R}} \quad (8)$$

where, R is the reflectance of the films.

The electrical characterization was examined with the aid of Keithley 4ZA4 2400 sourcemeter equipped with a four-point probe setup, for measurement of voltage and current and other electrical properties were calculated using equations (9)-(12).

The sheet resistance, R_s of the films were obtained using the relation.

$$R_s = K\frac{\mathrm{V}}{\mathrm{I}} \quad (9)$$

where, K is a constant and is expressed as;

$$K = \frac{\pi}{\ln 2} = 4.533 \quad (10)$$

The resistivity (ρ) of the deposited films was calculated using equation (10);

$$\rho = R_s \times x\, t \quad (11)$$

And the conductivity (σ) was determined using the relation,

$$\sigma = \frac{1}{\rho} \quad (12).$$

3. Results and Discussion

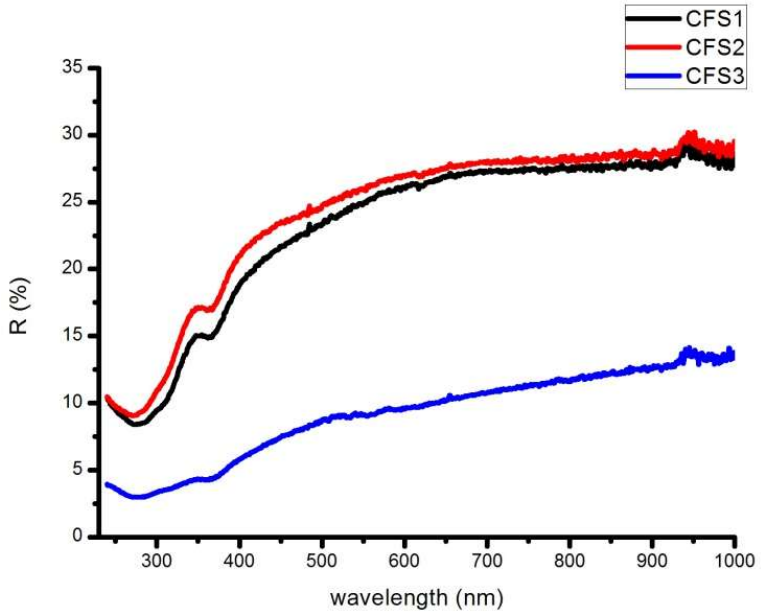

Fig. 1: Reflectance versus wavelength of thin film samples: CFS1, CFS2, and CFS3.

The reflectance graph for the deposited thin films is shown in Fig. 1, with the sample deposited at 40 cycles having the highest value of 30%, followed by the sample deposited at 30 cycles having 25.7% while the sample deposited at 50 cycles has the least value of 14% in the near infrared region (NIR). It is observed that these values decrease down the electromagnetic spectrum through the visible (VIS) to the ultraviolet (UV) regions. This provides wide latitude for the applications of the thin film. Average reflectance was found to be below 35% for all films. The grown film is a useful material for the window layer part of solar cells and also for screening off UV radiation that is harmful to human beings and animals, as reported by K.S. Wanjala et al., that it is imperative for reflectivity to be as low as possible

for solar applications [10]. It was observed from the transmittance graph (Fig. 2) that for wavelengths above 500 nm the deposited films at 30 and 40 cycles have the highest transmittance of 85% and 91%, respectively, followed by the sample deposited at 40 cycles with 71% transmittance. The transmittance varies most times as the SILAR cycle and at other times is inversely proportional. In all the films below 450 nm there was a sharp

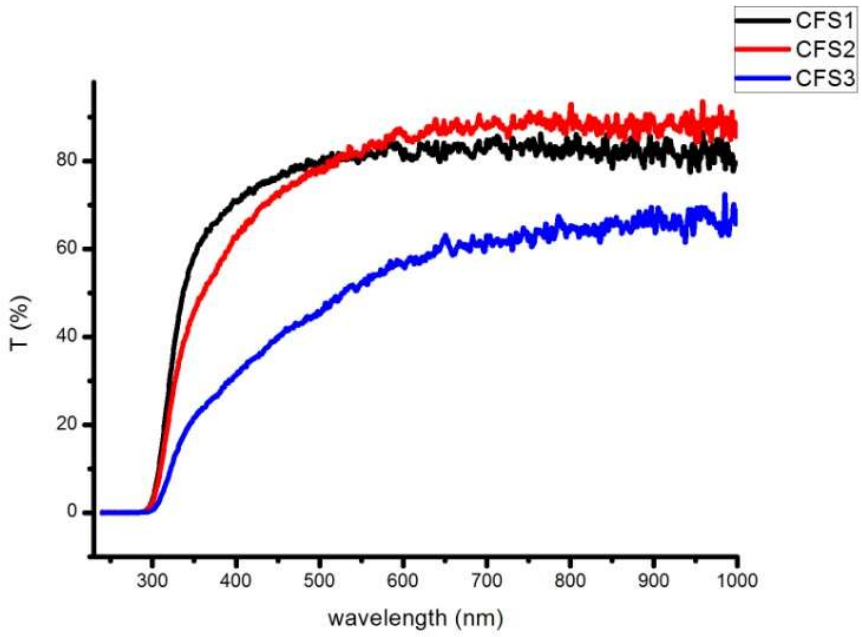

Fig. 2: Transmittance versus wavelength of thin film samples: CFS1, CFS2, and CFS3.

fall in the percentage transmittance of the thin films, which indicates an increase in photon absorption [5]. As shown on the graph, the average transmittance at wavelength (λ) = 800 nm was found to be between 80% and 91%. These values of fairly low and high transmittances in UV and VIS-NIR regions, respectively, are in agreement with the previous research reports [3, 9] that employed CBD to fabricate the same thin film and reported the same for its optical and solid-state properties. However, the high values suggest the suitability of the films for window layers in solar cells. From the optical absorption spectra of the thin films shown in Fig. 3, it was observed that all the deposited samples exhibited high absorbance in the UV region of the electromagnetic spectrum between wavelengths of 250 nm and 300 nm. Meanwhile, the absorbance of the thin film was between 2.6 and 5.3. The increase in absorption occurs when the photon energy (hν) reaches the value of the energy gap (E_g) where electronic transfers occur between the valence band and conduction band. The film shows relatively low absorbance in the NIR regions of the spectrum (less than 1.0). This aligns with the reports of [3, 5 and 9] as they also observed similar results in the UV region and low absorbance in the VIS-NIR region in their experiments

using CBD and

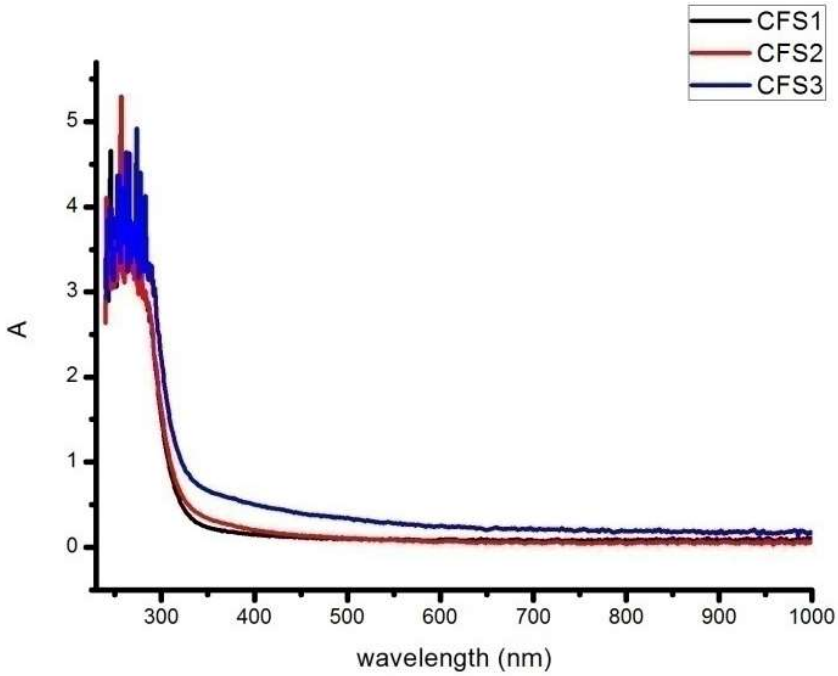

Fig. 3: Absorbance versus wavelength of thin film samples: CFS1, CFS2, and CFS3.

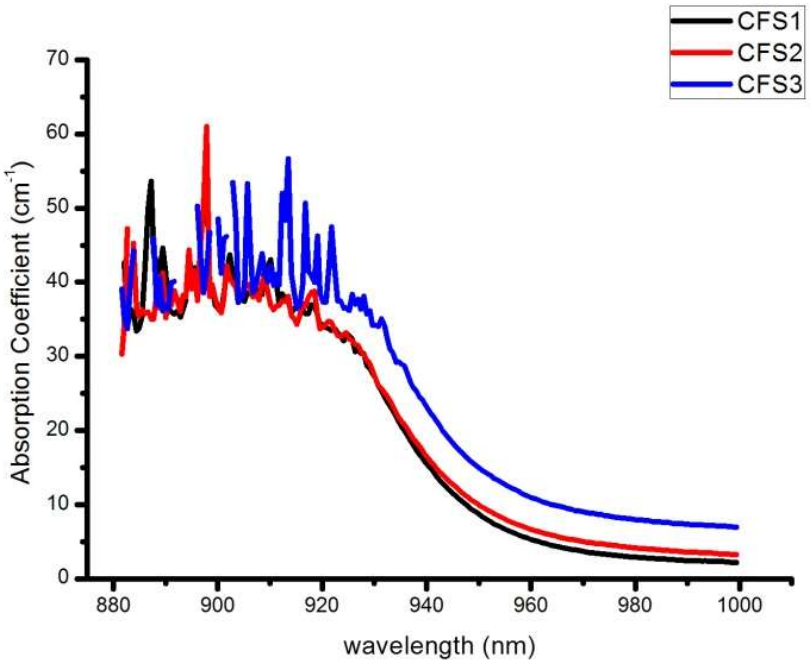

Fig. 4: Absorption coefficient versus wavelength for the deposited thin film samples: CFS1, CFS2, and CFS3.

SGT, respectively. Fig. 4 is the graph of the absorption coefficient as a function of wavelength for the deposited thin films. The graph of the figure showed that the deposited thin films have a very

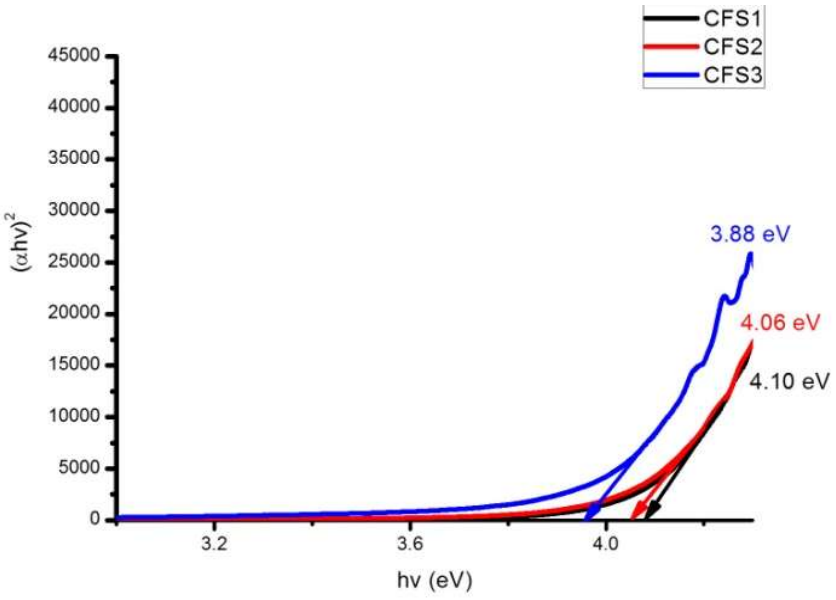

Fig. 5: Tauc plot for the deposited thin film samples: CFS1, CFS2, and CFS3.

high absorption coefficient in the wavelength range of 880-920 nm, which will enable them to absorb effectively or completely a range of incoming spectrum so more electron hole pairs are generated and more electrical energy is produced. It can be observed from the figure that the values of the absorption coefficient for all the films are very close to zero for wavelengths above 940 nm. The absorption coefficient of the films increased with an increase in SILAR cycle. In order of increasing SILAR cycle, the energy band gap (E_g) of 4.10 eV, 4.06 eV and 3.88 eV were obtained from the Tauc plot for direct allowed transition (Fig. 5), through the intercept on hν-axis after extrapolation of the straight-line section in the high-energy region of the plot. It is observed from Fig. 6 that the E_g values decreased as the SILAR cycle increased. This is in agreement with the result reported by Q.A. Adeniji et al., [5]. The band-gap of the window layer should be high and the layer be thin as possible to maintain low series resistance to ensure the window layer does not absorb any of the incident light and to allow maximum photon energy to reach the absorber layer where it is needed for the generation of electrons [5]. Graph of extinction coefficient as a function of wavelength for the thin films is plotted in Fig. 7. The extinction coefficient values show a similar

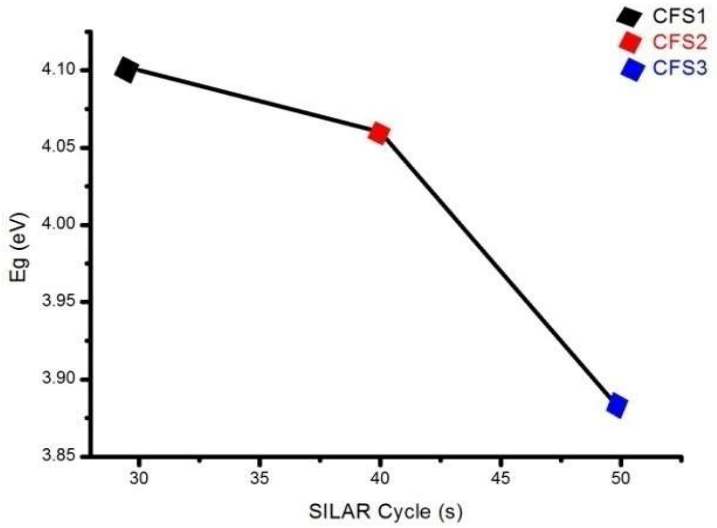

Fig. 6: Variation of E_g with the SILAR cycle of the deposited thin film samples: CFS1, CFS2, and CFS3.

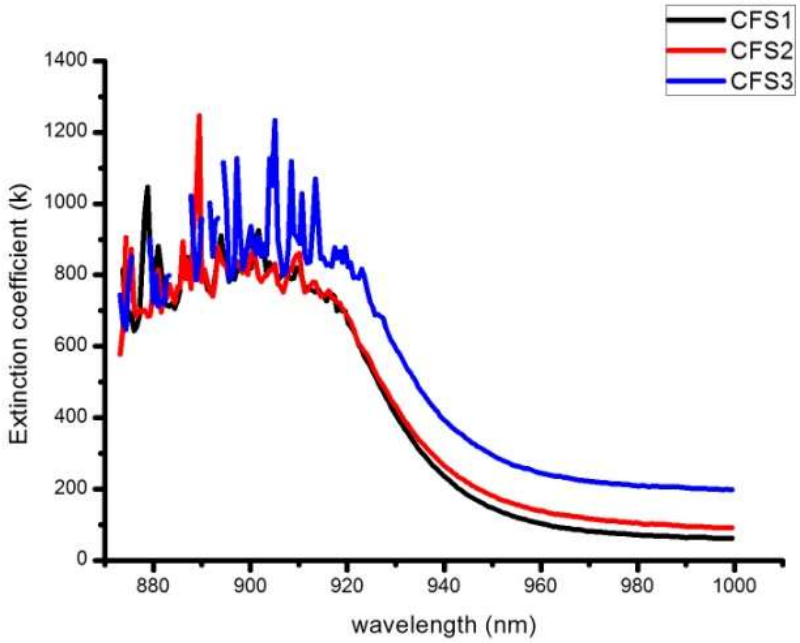

Fig. 7: Extinction coefficient versus wavelength for the deposited thin film samples: CFS1, CFS2, and CFS3.

trend as the absorption coefficient. It can be observed from the figure that the values of the extinction coefficient for all the films are very close to zero for wavelengths 940 nm and above. The extinction coefficient of the films increased with an increase in SILAR cycle. The refractive

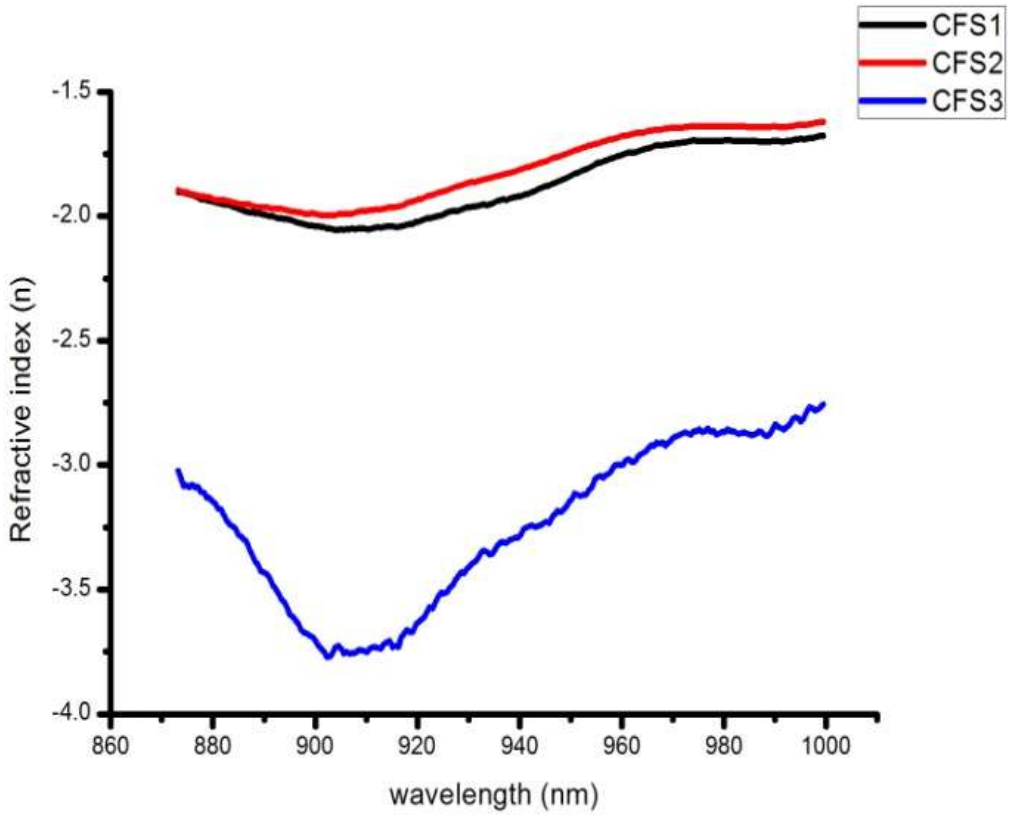

Fig. 8: Refractive index versus wavelength for the deposited thin film samples: CFS1, CFS2, and CFS3.

index dispersion plays a prominent part in the research of optical materials, because it is a major factor in optical communication and in designing devices for spectra dispersion [6]. The graph of the refractive index against wavelength for the deposited thin films is displayed in Fig. 8. The figure indicates that there was no refractive index in the UV-VIS regions for all the films. It is clear from the figure that the refractive index of the films initially decreased as wavelength increased up to 915 nm then increases as the wavelength increased in the NIR region. It can also be observed from the figure that the maximum values of the refractive index for all the films falls at a wavelength of about 975 nm and the values are -1.70, -1.60, and -2.85 in increasing order of SILAR cycle. The CFS thin films is a different kind of semiconductor material that exhibited varying negative refractive indices which shows that photon energy travelling through the deposited thin film materials is refracted in the opposite direction as photon energy in a normal material owing to the fact that negative index metamaterial causes light to refract differently than

Table 1: Electrical results of the thin film samples

Sample Code	Voltage (v)	Current (A)	Sheet resistance, R_s (Ωm^{-2})	Resistivity $(\Omega m)^{-1}$	Conductivity (Ωm)
CFS1	3.637×10^{-1}	2.126×10^{-8}	7.752×10^{7}	1.550×10^{7}	6.451×10^{-8}
CFS2	3.699×10^{-1}	4.112×10^{-8}	4.077×10^{7}	8.154×10^{6}	1.226×10^{-7}
CFS3	2.139×10^{-1}	3.319×10^{-8}	2.921×10^{7}	5.841×10^{6}	1.712×10^{-7}

common positive index material [11].

Table 1 showed that the conductivity of the grown thin film varied from 6.450 x 10^{-8} $(\Omega m)^{-1}$ to 1.712 x 10^{-7} $(\Omega m)^{-1}$ in increasing order of SILAR cycle. This enhances the electrical property of the film and makes it a good material for solar cell applications. Resistivity should not be too high or too low due to the inevitable defects in solar cells during the actual production process [5]. The electrical conductivity results revealed that as the SILAR cycle increased, the conductivity of the deposited films was also found to increase.

IV. Conclusion

In this study, the synthesis and characterization of CFS thin films have been successfully achieved through SILAR technique from the aqueous solution of $Fe(NO_3)_3.9H_2O$, $CuCl_2.2H_2O$, and $(NH_2)_2CS$), EDTA, TEA, NH_4OH, and deionized water. The results obtained revealed that the energy band gap values of the thin films decreased as the SILAR cycle increased. As SILAR cycles increased, other solid-state properties of the films were affected. This provides a wide range of applications of the thin films in solar cell fabrication, screening off UV radiation that is harmful to human beings and animals due to its high absorbance, low transmittance and low reflectance in the UV region, coating of poultry buildings, eye glasses coating, solar thermal conversion, solar control, anti-reflection coating, and window layers in solar cells. Anticipation is that the growing of the thin film with a specific molar concentration of the precursors higher than 0.7 *M* will lead to more applications of the ternary material.

Acknowledgements

The authors are thankful to the Department of Physics, Olabisi Onabanjo University, Ago-Iwoye, Nigeria, for creating an enabling environment for this study.

- **No conflict of interest among authors.**
- **This article is not funded by any organization or institution.**

References

- Odunaike, K, Adeniji, Q. A., Sheu, A. L., Fowodu, T. O., and Alabi, T. A. (2021). Effect of Different SILAR cycle on Chemically Deposited Zinc Copper Sulphide (ZnCuS). Int. J. Thin. Fil. Sci. Tec. **10(2)**, 117-120.
- Ezenwa, I. A. and Okoli, L. N., (2015). Synthesis and Characterization of Chemically Deposited Iron Copper Sulphide (FeCuS) Thin Films. Asia Pacific Journal of Research, I(XXI); 14-21. ISSN: 2320-5504, E-ISSN-2347-4793
- Obasi, B. I., Osuwa, J. C. and Odu, D. A. (2016). Effects of Varying Copper (Cu) Ion Concentrations of Ternary Compound of Copper Iron Sulfide (CuFeS) Thin Films. International Journal of Science and Technology, 5(8); 369-373.
- Uhuegbu, C. C. (2010). Solution growth technique for iron copper sulphide ternary thin film and its optical characteristics. Am. J. Sci. Ind. Res., 1(3); 392-396. ISSN: 2153-649X. DOI:10.5251/ajsir.2010.1.3.392.396
- Adeniji, Q. A., Odunaike, K, Fowodu, T. O., and Talabi, A. T. (2020). Influence of SILAR cycle on the Energy bandgap of Iron Copper Sulphide (FeCuS) Thin Films deposited on SLG Substrate. NanoWorld Int. J. **5(4)**, 49-52.
- Osanyinlusi O. and Aregbesola A. E. (2021). Optical Properties of Cadmium Sulphide (CdS) Thin Films Spin-Coated on Glass Substrates. Jordan Journal of Physics, **14(1)**; 49-58. *Doi:* https://doi.org/10.47011/14.1.5
- Ivanauskas, A., Ivanauskas, R. and Ancutiene, I. (2021). Effect of In-Incorporation and Annealing on Cu_xSe Thin Films. Materials,14; 3810. https://doi.org/10.3390/ma14143810.
- Nwori1, A.N., Ezenwaka, L.N., Ottih, I.E., Okereke, N.A., Umeokwona, N.S., Okoli, N.L. and Obimma, I. O. (2021). Study of the Optical and Solid-State Properties of Copper Manganese

Sulphide (CuMnS) Thin Film Semiconductors for Possible Optoelectronics Applications. Journal of Physics and Chemistry of Materials, **8(3)**; 23-33. E-ISSN: 2348-6341.

- Okoli, N. L., Udechukwu, I. E. and Okpaneje, O. T. (2016). Effect of Deposition Time on Optical and Solid State Properties of Chemically Deposited Iron Copper Sulphide (FeCuS) Ternary Thin Films. African Journal of Education, Science and Technology, 3(1); 71-80. ISSN: 2309-9240.
- Wanjala, K. S., Njoroge, W. K. and Ngaruiya, J. M. (2016). Optical and Electrical Characterization of ZnS:Sn Thin Films for Solar Cell Application. International Journal of Energy Engineering. 6(1); 1-7. p-ISSN: 2163-1891. doi:10.5923/j.ijee.20160601.01
- Veselago, V., Braginsky, L., Shklover, V and Hafner, C. (2006). Negative Refractive Index Materials. Journal of Computational and Theoretical Nanoscience, (2): 1-30.